Fatigue Life Assessment of 5083 "O" Aluminum Alloy Joints Welding by The MIG Process

Gabriela Pegoretti[a], William Haupt[b]*, Alexandre Pereira Dall Oglio[a], Kaue Correa Riffel[c], Charles Leonardo Israel[d]

[a,c]*Faculty of Engineering and Architecture. Welding Technology Laboratory University of Passo Fundo, BR 285 São José, Passo Fundo, CEP: 99052-900 Rio Grande do Sul, Brazil*

[b]*Postgraduate Program in Design and Manufacturing Processes PPGPPF / UPF. Welding Technology Laboratory University of Passo Fundo, BR 285 São José, Passo Fundo, CEP: 99052-900 Rio Grande do Sul, Brazil*

[d]*Federal University of Santa Catarina, Department of Mechanical Engineering, Welding Laboratory, Florianópolis, Santa Catarina, Brazil*

[e]*Postgraduate Program in Design and Manufacturing Processes PPGPPF / UPF. Metallography Laboratory University of Passo Fundo, BR 285 São José, Passo Fundo, CEP: 99052-900 Rio Grande do Sul, Brazil*

[a]*Email: 106904@upf.br , [b]Email: williamhaupt@upf.br, [c]Email: 150747@upf.br, [d]Email: kaue.riffel@posgrad.ufsc.br, [e]Email: Israel@upf.br*

Abstract

In order to analyse the fatigue resistance of joints welded by the MIG process in aluminium alloy 5083 "O", the present study analyses the influence of the shielding gases used during welding in the final strength of the product when it is subjected to fatigue stresses. The welds were made using two gas configurations, the first configuration being with 100% argon and the second with 75% argon and 25% helium. The results indicate that with the use of 25% helium compared to 100% argon it is possible to reduce the porosity present in the melted area of the joints and increase fatigue life for the conditions with cyclical loads of 80 and 60% of the maximum tension of the materials.

Keywords: Automatic MIG welding; Aluminium 5083 "O"; Fatigue life welds; Fractography.

----

* Corresponding author.

1. Introduction

The aluminium and its alloys are widely used on the assembly lines of various industrial sectors, such as automotive, aviation and shipbuilding due to its easy and cheap acquisition, in addition to having good thermal and electrical properties, low density and good resistance to corrosion [1]. The choice of alloys applied to each project, as well as the joining processes used, depends on the field of application in which they will be used [2]. The Al alloys of grades 5XXX (Al-Mg) and 6XXX (Al-Si-Mg) are widely used in the construction of structures, vehicle manufacturing, pressure vessels and marine industry. Various welding processes can be applied to these high quality alloys, the preferred methods being arc welding with inert gas (MIG), welding with inert gas and tungsten electrode (TIG) and linear friction welding (FSW) [2,3]. The MIG welding process stands out for its high welding speed, penetration of the weld bead deposited and productivity, having as negative points the pronounced growth of grains in the region of the thermally affected zone, high distortion due to the great heat contributed, presence of pores and cracks resulting from the solidification of the melt pool. The TIG and FSW processes have higher metallurgical quality with less distortions in the structures, however the productivity is usually well below that achieved in MIG welding. Usually, the MIG welding process is preferred for aluminium alloys due to its simplicity, speed and possibility of automation, reaching high production speeds in the series manufacture of structures [3,4]. However, studies report the strong presence of defects such as the presence of pores and cracks in conventional MIG welding of aluminium alloys. Although there are no fully efficient methods for resolving these defects, studies by [5,6,7,8] report that the use of current pulses with CC + electrode allows the refinement of grain in the welding of Al alloys, reducing the incidence of pores and improving the resistance to cracking. It is also reported in the studies of [7,8] that the use of He gas in mixture with Ar gas allows longer solidification interval with less pore incidence in the molten region, it is also possible to increase the welding speed due to the greater heat generated in the welding. This study examined the effects of adding 25% helium to argon gas for pulsed MIG welding of the annealed 5083 "O" alloy. The macrostructures of the joints were examined, the behaviour of the hardness in its cross section and the fatigue life of the joints for loads of 80, 60 and 40% of the maximum stresses obtained by the base material. Finally, fracture surfaces after fatigue tests were investigated by scanning electron microscopy (SEM).

2. Materials and methods

2.1 Welding Procedure

In the present work, Al/Mg 5083 "O" alloy plates with a thickness of 6.35mm were prepared. The dimensions of the welded materials and the geometry of the joints used are shown in Figure 1.

The welding of the materials was carried out by the welding robot SUMIG AF - 4011 with the OTC DP-400 inverter power source. The application of automatic welding allows an adequate control of the parameters during welding. The ER5183 was used as a filler material, with a diameter of 1.2mm, with the welding being carried out with a pulsed current of average value 150 A, welding speed of 500mm/min, shielding gas flow of 10l/min, displacement angle of 20° and with the welding torch being pulled. To perform the welds, the welding surfaces were properly cleaned with acetone and ceramic backing was used to support the formation of the joint

root, as seen in Figure 2.
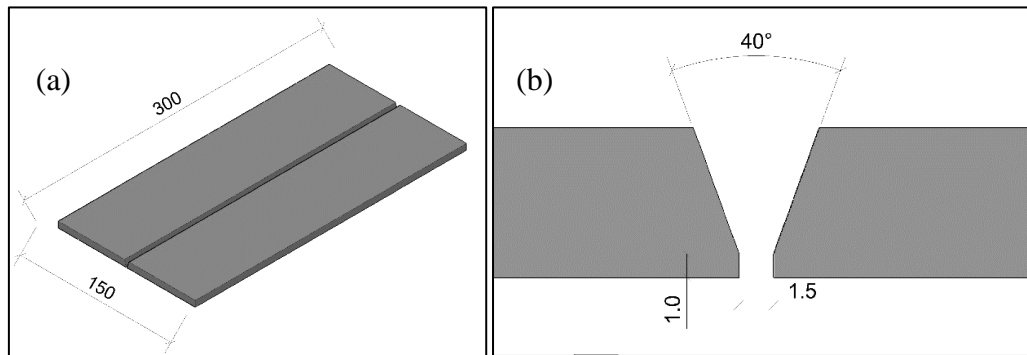
Figure 1: (a) Dimensions of welded specimens; (b) Geometry of the chamfer used in welding.

Figure 2: Fixing and backing device for the joint root support.

The variable analysed in the study was the composition of the shielding gas, with a set of joints done with Ar as a shielding gas and another set with Ar+25%He.

2.2 Macrostructural characterization and microhardness

The macrostructural characterization was performed in the cross section of the joints, with the samples being prepared by refrigerated cutting for extraction, resin inlay, sequential sanding with sandpaper # 220, 400, 600, 1200 and 2500, polishing with 1μm diamond solution and chemical attack with regal water reagent containing 30ml of HCl, 60ml of absolute alcohol and 1ml of HNO3. After analysing the macrostructures of the joints, they were again sanded and polished in the same way as before to make the microhardness profiles. The equipment used was a Shimadzu microdurometer model HMV-G20ST, with 0.3kgf test loads and distance between indentations of 0,5mm, following the procedures of the standard ASTM E 384-08 [9]. Two profiles were made, one next to the face of the joints and the other next to the root of the joints.

2.3 Tensile and fatigue tests

For the joint fatigue, tests 3 specimens were previously uniaxially tensile tested, according to the ASTM E8M-04 [10] procedure, with an average maximum tension of 258MP±21. The tests were performed on a Shimadzu Servopulser with 10kN of maximum load capacity. From the maximum tension, the parameters for the uniaxial fatigue test were defined. The tests were performed on the same equipment used for tensile tests, with its

programming for dynamic loading in tensile regime. In the test, three specimens were evaluated per condition, with the test loads being defined as 80%, 60% and 40% of the maximum tension of the base material. The fatigue ratio used was 0.1 and the frequency was 15 Hz, with the tests being carried out in an uncontrolled environment. Fatigue tests followed the procedures of the ASTM E466-07 [11] standard, as shown in Figure 3.
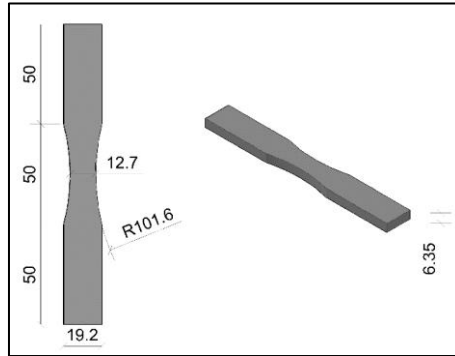

Figure 3: ASTM E466 fatigue specimens.

After the fatigue test, analyses were performed using a scanning electron microscope (SEM) in the fatigue crack initiation region, with the evaluation of points that were responsible for the nucleation of the defects.

3. Results and Discussion

3.1 Macrography and Microhardness

The Figure 4 (a) shows a larger fused area for the sample welded with Ar+25%He compared to Figure 4 (b). This fact can be explained by the greater calorific power of the gas mixture, creating a larger melted region with a greater dilution of the base material. There is also a significant reduction in the pores formed, this fact is attributed to the greater calorific power of the shielding gas that allows a longer solidification interval, thus causing a greater diffusion of gases and reduction of pores. When comparing the macrographs of the welds, it is possible to visualize the greater presence of pores in the weld section with 100% Ar gas, as seen in Figure 4 (b).
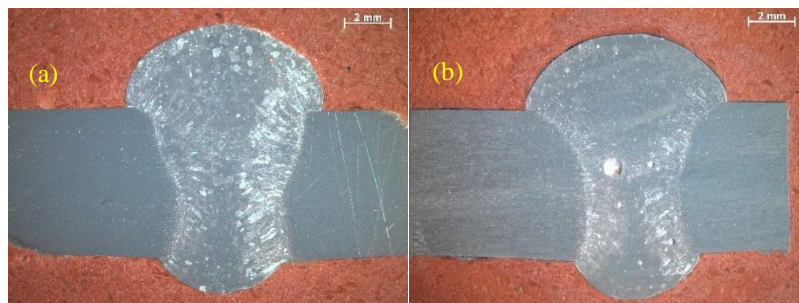
Figura 4: Macrographs (a) Ar+25%He and (b) Ar.

The microhardness values obtained from the base material were 80±5HV. After welding with Ar+25%He it is possible to verify a uniformity in the hardness values, being that the reduction was registered only in the region

fused to the root with a slight reduction in the hardness of the cord face. In the condition of welding with Ar gas, there was a strong variation, showing hardness drop points. The Figures 5 (a) and (b) show the position and graphs of microhardness profiles for the Ar+25%He and Ar welds respectively.
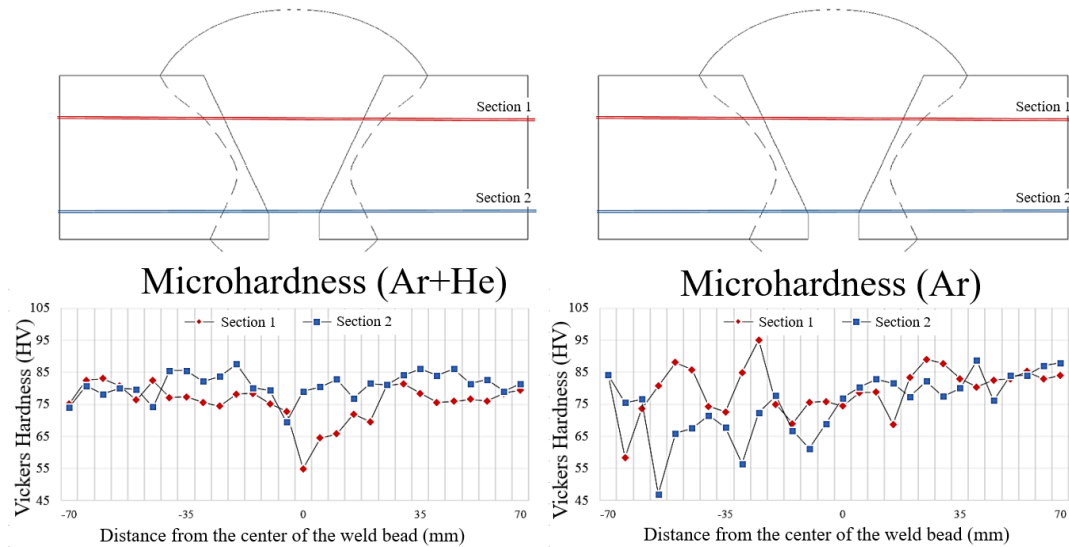
Figure 5: (a) Ar+He weld microhardness profiles and (b) Ar weld microhardness profiles.

3.2 Fatigue Tests

The results of the fatigue tests are shown in Figure 6 and show the best behaviour of the joint welded with Ar+25%He gas, with the greatest number of cycles for failure at loads of 80 and 60% of the maximum tension. In the load condition, all joints did not fail after $1x10^6$ cycles, being considered infinite life in fatigue for the maximum tension of 103MPa or 40% of the maximum tension.
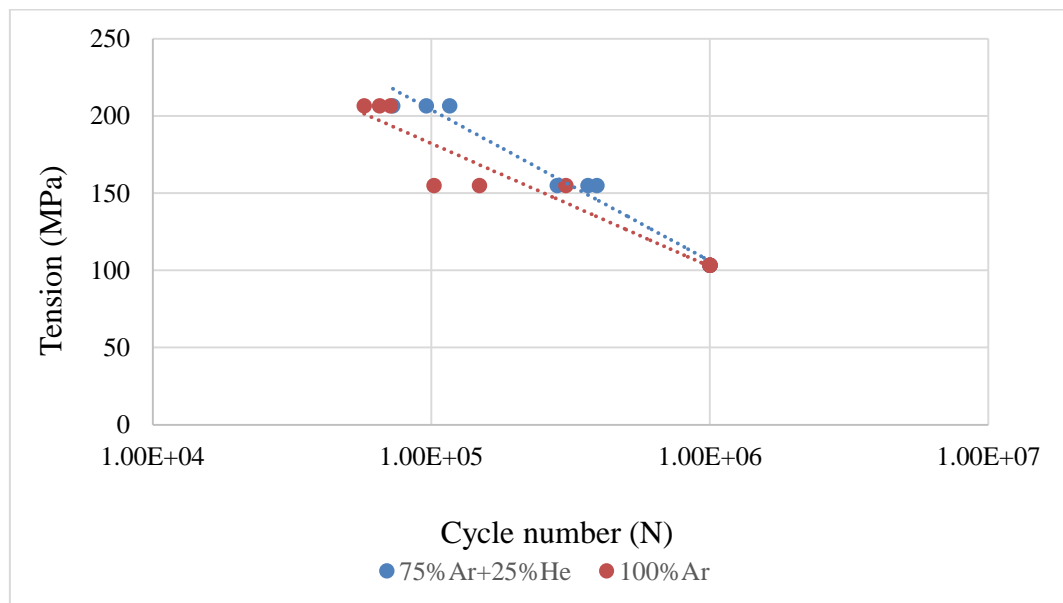

Figure 6: Results of the fatigue tests.

3.3 Fractographies Fatigue Tests

The fracture surfaces of Figures 7 (a) and (b) show, in different magnifications, the nucleation region of the fatigue failure that occurred for 80% of the maximum tension with Ar+25%He gas. In the Figure 7 (b) it is possible to see the presence of dark spots marked by arrows showing the possible presence of inclusions. The Figures 7 (c) and (d) show the fracture surface for the same condition with a maximum fatigue load of 60% of the maximum tension. The crack nucleation region is indicated by an arrow in the Figure 7 (c), being verified in Figure 7 (d) the presence of defects that provided the nucleation of the fracture. The Figures 7 (e) and (f) show the condition using Ar gas with 80% of the maximum fatigue tension, becoming evident the crack nucleation in a region with a strong presence of pores. This is due to the greater formation of pores in the fused region with the use of Ar gas. The pores are indicated by arrows in the figures. Figures 7 (g) and (h) show the fracture surface in the same condition with 60% of the maximum load applied in fatigue, showing the initiation of fatigue cracks in a region with coarse porosity.
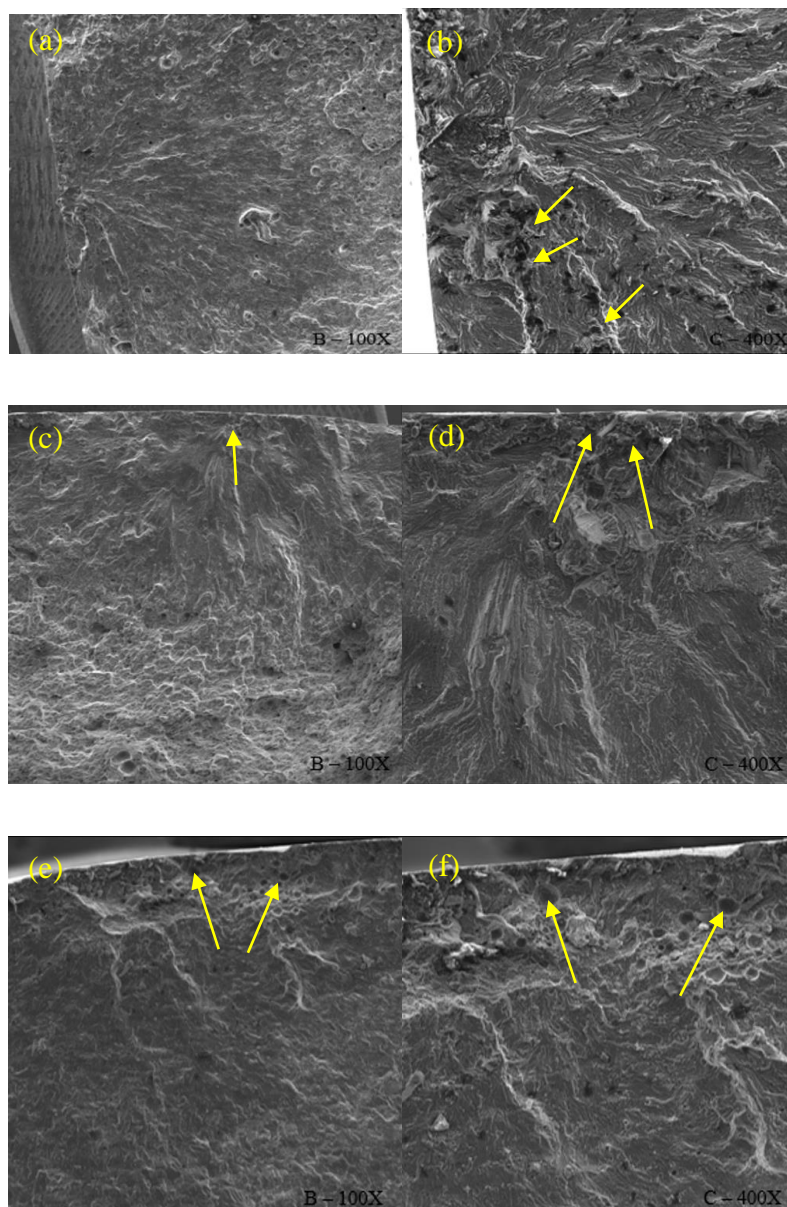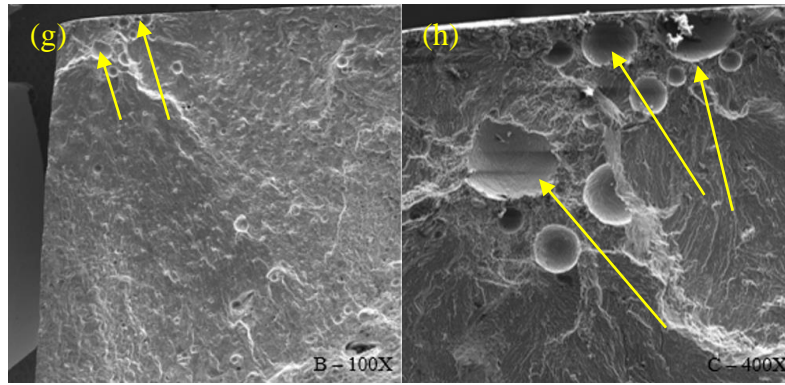
Figure 7: Fracture surfaces of fatigue samples. (a) and (b) Ar+25%He with 80% of the maximum tension; (c) and (d) Ar+25%He with 60% of the maximum tension; (e) and (f) Ar with 80% of the maximum tension; (g) and (h) Ar with 60% of the maximum tension.

The Figure 8 (a) shows the composition map of the fracture onset region for the condition using Ar+25%He with 80% of the maximum fatigue tension. The dark spots mentioned in the fractographic analysis appear on the map as rich in Fe/Al and oxygen, indicating that the fracture nucleation occurred in a region with the presence of iron oxide inclusions. Figure 8 (b) shows the composition map of the fracture region in the condition using Ar with 80% of the maximum fatigue tension. Its composition of the fracture surface is quite uniform, not showing the presence of inclusions, corroborating the assessment that the cracks were nucleated in regions with a large presence of pores.
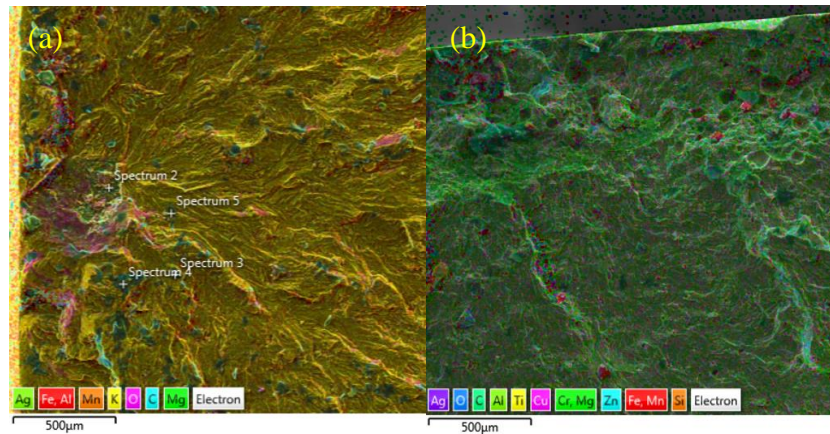
Figura 8: Composition maps made by SEM of fatigue fractures. (a) Ar+25%He with 80% of the maximum tension; (b) Ar with 80% of the maximum tension.

3.4 Discussion of the Results

The work illustrated that the use of the gas mixture Ar +25%He allowed a lower incidence of pores in the molten region, compared to welding with 100% Ar, being also possible to verify the greater dilution of the base material with the use of the gas mixture. This fact is attributed to the greater calorific power presented by the addition of He gas to the mixture, modifying the solidification interval allowing a greater diffusion of gases out

of the molten region, causing less pore formation in the weld bead. Better heat distribution during welding, provided welds with greater uniformity of hardness and an area with little presence of pores. With this, it is possible to verify through the fatigue test that the welds made with the mixture Ar+25%He presented a longer life in fatigue for the same level of tension of the welding with 100% Ar. The closer to the maximum mean stress, the greater the disparity between the number of cycles resulting from the use of the two gases. The fractographs allow us to conclude that for the welding condition with Ar+25%He, there was a nucleation of cracks near oxide inclusions and small defects, with little porosity, and in the condition of welding with 100% Ar, however, it is possible to observe the nucleation of the fatigue failure along regions with relatively large pores. The welding condition with 100% Ar provided the formation of pores, with fatigue cracks being nucleated next to colonies of pores generated in the solidification of the welding bead. For the condition with Ar+ 25% He, a reduction in the number of pores and generation of iron oxide inclusions, responsible for the formation of the nucleation region of the fatigue cracks, was observed. It is also possible to verify a better performance of the joints obtained with the gas mixture Ar + 25% He, due to the reduction in the formation of porosities. It is possible to verify that all welds presented infinite fatigue life for stresses of 40% of the maximum tension, with the criterion of the $1x10^6$ cycles being applied, being indicated the application for cyclic tensile tension values below 40% of the breaking tension of the base material.

4. Conclusions

With this study it was possible to conclude that:

The use of the gas mixture Ar+25%He allowed a lower incidence of pores near the fused region of the joints compared to welding using 100% Ar. MIG welds in the aluminium alloy 5083 "O" using the gas mixture of Ar+25%He allows greater fatigue life for stresses of 80 and 60% of the maximum tension of the base material compared to welds made using 100% Ar. The high incidence of pores in welding with 100% Ar allowed the nucleation of fatigue cracks, accelerating the failure for this welding condition. With the welding using Ar+25%He it was possible to verify that the beginning of the fracture occurred in points with the presence of oxide inclusions and small intrusions, not being related to the formation of pores for this welding condition.

5. Recommendations

This proposed analytical methodology aims to evaluate the application of these unions in the automobile industry, construction of special vehicles, structures subjected to cyclical loading and agricultural machinery. The work indicates strong benefits in the use of the gas mixture Ar+25%He, being indicated for use when looking for better quality of joints, with less pore incidence and longer life in fatigue.

References

[1]. L. Anhua, T. Xinhua, L. Fenggui. "Study on welding process and prosperities of AA5754 Al-alloy welded by double pulsed gas metal arc welding". Materials & Design, vol. 50, pp. 149–155, 2013.

[2]. E. Çetkin, Y.H. Çelik, S. Temiz. "Effect of welding parameters on microstructure and mechanical properties of AA7075/AA5182 alloys joined by TIG and MIG welding methods". Journal of the

Brazilian Society of Mechanical Sciences and Engineering, vol. 42, 2020.

[3]. G. Mathers. The welding of aluminium and its alloys. Sawston, CAM. Woodhead publishing, 2002.

[4]. I. Sevim, F. Hayat, Y. Kaya, N. Kahraman, S. Şahin. "The study of MIG weldability of heat-treated aluminum alloys". The International Journal of Advanced Manufacturing Technology, vol. 6, pp. 1825-1834, 2013.

[5]. N. Fuheng, D. Honggang, C. Su, L. Peng, W. Leyou, Z. Zhouxing, L. Xintao, Z. Hai. "Microstructure and mechanical properties of pulse MIG welded 6061/A356 aluminum alloy dissimilar butt joints". Journal of materials science & technology, vol. 34, pp. 551-560, 2018.

[6]. J.C. Dutra, R.H.G.e. Silva, B.M Savi, C. Marques, O.E. Alarcon. "New methodology for AC-pulsed GMAW parameterization applied to aluminum shipbuilding". Journal of the Brazilian Society of Mechanical Sciences and Engineering, vol. 38, pp. 99-107, 2016.

[7]. H. Guo, J. Hu, H.L. Tsai. "Formation of weld crater in GMAW of aluminum alloys". International Journal of Heat and Mass Transfer, vol. 52, pp. 5533-5546, 2009.

[8]. O.I. Oluwole; O.J. Ajibade. "Effect of welding current and voltage on the mechanical properties of wrought (6063) aluminium alloy". Materials Research, vol. 13, pp. 125-128, 2010.

[9]. ASTM E384, Standard Test Method for Microindentation Hardness of Materials, ASTM International, West Conshohocken, PA, 2008.

[10]. ASTM E8M-04, Standard Test Methods for Tension Testing of Metallic Materials, ASTM International, West Conshohocken, PA, 2008.

[11]. ASTM E466, Standard Practice for Conducting Force Controlled Constant Amplitude Axial Fatigue Tests of Metallic Materials, ASTM International, West Conshohocken, PA, 2007.

Acknowledgements